ECOS 2011: Optimal Concentration and Temperatures of Solar Thermal Power Plants

Ronan K. McGovern[a,b], William J. Smith[a]

[a] *Department of Mechanical Engineering, University College Dublin, Ireland.*
[b] *Department of Mechanical Engineering, Massachusetts Institute of Technology, Cambridge, USA, mcgov@mit.edu,* ***CA***

Abstract:

Using simple, finite-time, thermodynamic models of solar thermal power plants, the existence of an optimal solar receiver temperature has previously been demonstrated in literature. Scant attention has been paid, however, to the presence of an optimal level of solar concentration at which the conversion of incident sunlight to electricity (solar-to-electric efficiency) is maximized. This paper addresses that gap. The paper evaluates the impact, on the design of Rankine-cycle solar-trough and solar-tower power plants, of the existence of an optimal receiver temperature and an optimal level of solar concentration. Mathematical descriptions are derived describing the solar-to-electric efficiency of an idealized solar thermal plant in terms of its receiver temperature, ambient temperature, the receiver irradiance (radiation striking unit receiver area), solar receiver surface to working fluid conductance, condenser conductance, solar collector efficiency, convective loss coefficients and radiative loss coefficients. Using values from the literature appropriate to direct-steam and molten-salt plants, curves of optimal solar receiver temperature, and optimal solar-to-electric conversion efficiency, are generated as a function of receiver irradiance. The analysis shows that, as the thermal resistance of the solar receiver and condenser increases, the optimal receiver temperature increases whilst the optimal receiver irradiance decreases. The optimal level of receiver irradiance, for solar thermal plants employing a service fluid of molten salts, is found to occur within a range of values achievable using current solar tower technologies. The tradeoffs (in terms of solar-to-electric efficiency) involved in using molten salts rather than direct steam in the case of solar towers and solar troughs are investigated. The optimal receiver temperatures calculated with the model suggest the use of sub-critical Rankine cycles for solar trough plants, but super-critical Rankine cycles for solar tower plants, if the objective is to maximize solar-to-electric efficiency.

Keywords: Concentration, Finite-time thermodynamics, Optimisation, Rankine, Solar thermal

1. Introduction

In many ways, the design and operation of solar thermal power generation systems is more complex and challenging than that of conventional fossil fuel power-plants. In addition to turbines, pumps, condensers and steam generators, technologies are required to concentrate, absorb and transfer solar thermal energy to the working fluid. The requirement of solar thermal plants to operate under transient conditions of insolation (incident solar radiation) imposes a further challenge on overall system design. Given the complexity of solar thermal power plants, the design of an optimised system is challenging, whether that optimisation be for cost or performance. Basic questions, which arise during the design process, include the following: What is the optimal top temperature of the working fluid? What is the optimal design level of solar concentration? These are the questions that guide us as we take the very first steps in designing a solar thermal power plant. Fortunately, it avers that extremely useful observations may be made by considering simplified system models of solar thermal facilities. The goal of this brief manuscript is elucidate the impact of geometric concentration and receiver temperature upon the performance of a Rankine cycle based solar thermal power plant.

1.1 Literature Review

The simplest embodiment of a solar thermal power plant has come to be known as the Mueser engine [1]. The system is modelled by a solar receiver exchanging heat with the sun and ambient surroundings according to the Stefan-Boltzmann law and a reversible Carnot heat engine operating between the hot thermal reservoir and a cold thermal reservoir at ambient temperature.

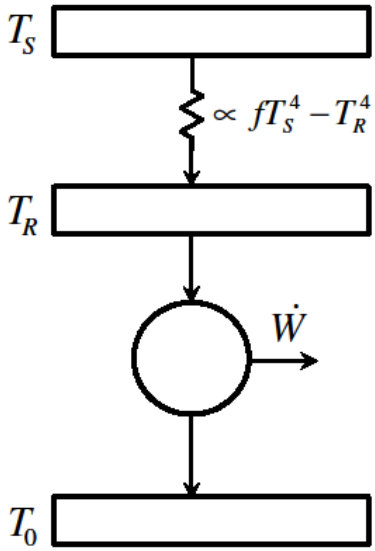

Fig. 1. Mueser engine

The Mueser engine illustrates the fundamental trade off between heat engine efficiency and minimization of radiative heat losses from the solar receiver. As the receiver temperature increases the Carnot efficiency increases whilst the radiative heat losses also increase according to the Stefan-Boltzmann equation for radiative heat transfer:

$$\dot{Q}_{rad} = \varepsilon_R A_R \sigma T_R^4, \qquad (1)$$

$$\eta_{Carnot} = 1 - \frac{T_0}{T_R}, \qquad (2)$$

The geometric concentration ratio, *X*, is defined as the ratio of solar collector to solar receiver area. The thermal efficiency, based on the first law of thermodynamics, is defined as the net power output per unit radiation incident upon the solar thermal power system.

$$\eta_{sys} = \frac{\dot{W}_{net}}{\dot{Q}_{in}}, \qquad (3)$$

Due to the presence of a fourth power heat transfer law, the optimisation of the system's thermal efficiency cannot be conducted analytically as is the case where linear heat transfer is involved [2-4]. By making an appropriate approximation for the effective sky temperature and using blackbody representations for solar, sky and ambient thermal reservoirs, De Vos [5] conducts numerical calculations to analyse various permutations of the Muser engine. Without geometric concentration De Vos finds that the maximum thermal efficiency achievable by a terrestrial solar thermal system is approximately 13%. With sunlight concentrated to the intensity at which it left the sun's surface (geometric concentration factor of 46 300), a theoretical thermal efficiency of 85.4% may be achieved. De Vos further builds upon this model and investigates the effect upon thermal efficiency of applying a theoretical bandgap material to the solar receiver surface, eliminating surface radiation above a specified wavelength and allowing an absorptivity of unity below that wavelength. At low levels of geometric concentration, thermal efficiency improves drastically with temperature, increasing from 13% to 52.6% for unitary concentration. At higher concentrations the optimal cutoff wavelength tends to infinity and the improvement is less significant.

Importantly, the Mueser model of a solar thermal plant cannot illustrate the existence of an optimal level of concentration. As concentration is increased, radiative losses will always decrease relative to the increased receiver irradiance. In practise however, a finite thermal resistance will exist between the solar receiver and the working fluid. In the case of a direct steam solar thermal power plant, this resistance will manifest itself in the heat transfer coefficient associated with the boiling of water within the solar receiver pipes. Navarrete-Gonzalez et al. [6,7] broached this matter and found that there appeared to be an optimal level of geometric concentration at which a solar thermal system's efficiency was maximised. What was not clear, however, was how this optimum affected real solar thermal plant designs.

2. Optimal Receiver Irradiance of Solar Thermal Plants

In this section, a simplified model of a Rankine cycle solar thermal power plant is developed based on previous work [1-8]. In our analysis, we choose to treat solar irradiation as an incident heat flux, specified as a rate of heat input per unit solar collector area, $\dot{q}_s$. Rather than considering the parameter of geometric concentration, we propose to instead consider receiver irradiance, I_R, defined as the heat flux striking unit solar receiver area. Receiver irradiance is thus the product of terrestrial insolation, collector efficiency and geometric concentration.

$$I_R \equiv \frac{Q_{in}}{A_R} = \frac{\dot{q}_s \eta_{coll} A_{coll}}{A_R} = \dot{q}_s \eta_{coll} X, \qquad (4)$$

Along with the receiver temperature, the value of receiver irradiance is an extremely important parameter in the thermal design of solar receivers. In addition, using receiver irradiance as a parameter avoids having to specify a level of incident terrestrial solar heat flux. Knowing the terrestrial heat flux at a specified location and given a design value of receiver irradiance, the geometric concentration factor required may be calculated. However, where one is concerned with cost optimisation, the value of geometric concentration may be more pertinent as it relates the size of the solar field to the receiver area.

The proposed model is that of a Mueser-Curzon-Ahlborn engine, with grey body receiver characteristics and convective cooling of the receiver surface.

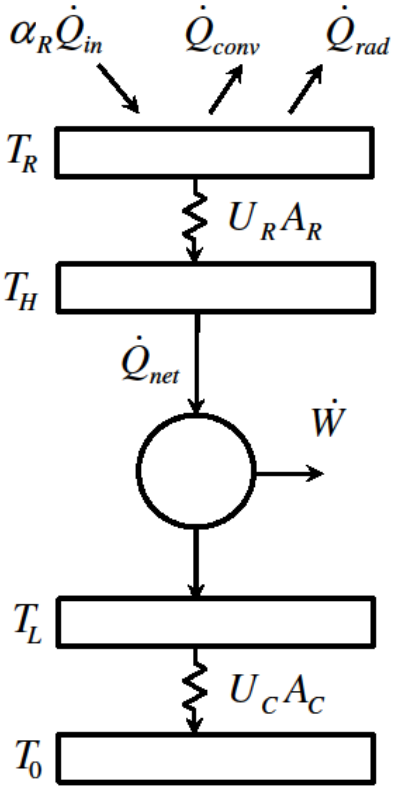

Fig. 2. Simplified solar thermal plant schematic

Solar radiation incident upon the receiver area is given by the product of collector efficiency, collector area and the level of solar irradiation per unit collector area. Radiative losses from the solar receiver are calculated using Stefan-Boltzmann's law and a grey body approximation. Convective losses are determined using appropriate correlations for the convective heat transfer coefficient.

$$\dot{Q}_{in} = \eta_{coll} A_{coll} \dot{q}_s , \qquad (5)$$

$$\dot{Q}_{rad} = \varepsilon_R A_R \sigma T_R^4 , \qquad (6)$$

$$\dot{Q}_{conv} = \bar{h}_{conv} A_R (T_R - T_0) , \qquad (7)$$

Heat transfer between the solar receiver and the high temperature working fluid and also between the low temperature working fluid and ambient temperature is given by linear heat transfer laws. (All heat transfer associated with the receiver is assumed to involve the same heat transfer area, A_R .)

$$\dot{Q}_{net} = U_R A_R (T_R - T_H) , \qquad (8)$$

$$\dot{Q}_C = U_C A_C (T_L - T_0) , \qquad (9)$$

The efficiency of the reversible heat engine is given by the Carnot efficiency:

$$\eta_{Carnot} = 1 - \frac{T_L}{T_H} , \qquad (10)$$

$$\dot{Q}_C = \frac{T_L}{T_H}\dot{Q}_{net}, \qquad (11)$$

Making use of Eq. 8-11 the following expressions are obtained for the ratio of low to high heat engine temperatures and the Carnot factor:

$$\frac{T_L}{T_H} = \frac{T_0}{T_R - Q_{net}\left(\frac{1}{U_R A_R} + \frac{1}{U_C A_C}\right)}, \qquad (12)$$

$$\eta_{Carnot} = 1 - \frac{T_L}{T_H} = 1 - \frac{T_0}{T_R - Q_{net}(R_R + R_C)}, \qquad (13)$$

The net rate of heat transfer into the heat engine is given by applying an energy balance to the receiver. For external tower or solar trough systems with high levels of geometric concentration, the incident radiation may be treated as solely coming from the collector area and not the surroundings. For cavity receivers heat radiated from adjacent walls is significant and a further term would be required in Eq. 14.

$$\dot{Q}_{net} = \alpha_R \dot{Q}_{in} - \dot{Q}_{rad} - \dot{Q}_{conv}, \qquad (14)$$

Taking the product of the net heat input to the Carnot engine and the Carnot efficiency, the rate of work obtained from the solar system is obtained. We wish to normalize this rate of work by the rate of heat input to the system to obtain a First Law efficiency:

$$\dot{W} = \dot{Q}_{net}\left(1 - \frac{T_L}{T_H}\right), \qquad (15)$$

$$\eta_{sys} = \frac{\dot{W}}{\dot{Q}_{in}}, \qquad (16)$$

Realizing that the receiver irradiance and the heat input to the system are linked by the collector efficiency and receiver and collector areas, an expression may be found for the efficiency of the solar thermal system as a function of the receiver irradiance and temperature.

$$I_R A_R \equiv \eta_{coll} A_{coll} \dot{q}_s = Q_{in}, \qquad (17)$$

$$\eta_{sys} = \eta_{coll}\eta_R\eta_{Carnot}, \qquad (18)$$

$$\eta_{sys} = \eta_{coll}\left[\alpha_R - \frac{\varepsilon_R \sigma T_R^4 + \bar{h}_{conv}(T_R - T_0)}{I_R}\right]\left[1 - \frac{T_0}{T_R - \dot{Q}_{net}(R_R + R_C)}\right], \qquad (19)$$

It is clear from Eq. 19 that as thermal resistances increase the Carnot efficiency will decrease. It is also clear that receiver efficiency can increase with increases in receiver irradiance. Furthermore an increase in the net rate of heat transfer into the heat engine also results in a decreasing Carnot efficiency. This explains why, in real solar thermal systems, the receiver irradiance cannot be increased indefinitely without compromising overall system efficiency.

3. Results

3.1 Optimal Receiver Irradiation

For an initial parametric study of a solar thermal system's efficiency, we set the collector efficiency, receiver absorptance and emissivity to unity. Convective cooling of the receiver is neglected and the receiver and condenser thermal resistances are set equal. The overall heat transfer coefficient within the receiver is taken to be 15 kWm^{-2}, a representative value for two phase boiling of water within a pipe [9]. The ambient temperature is set to 300 K.

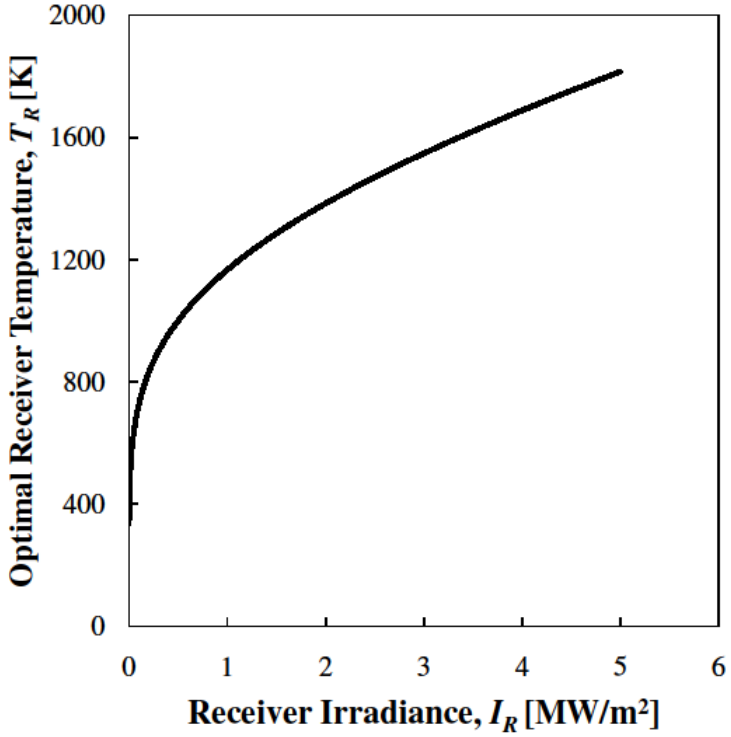

Fig. 3. Optimal receiver temperature versus receiver irradiance

As receiver irradiance increases, the optimal receiver temperature of a solar thermal system increases drastically. Optimal temperatures rapidly go beyond what is achievable with a sub-critical Rankine cycle, suggesting that alternative cycles such as Brayton or Stirling are required for optimal performance. Of course, the details of the required model (Fig. 2) will vary according to the choice of cycle.

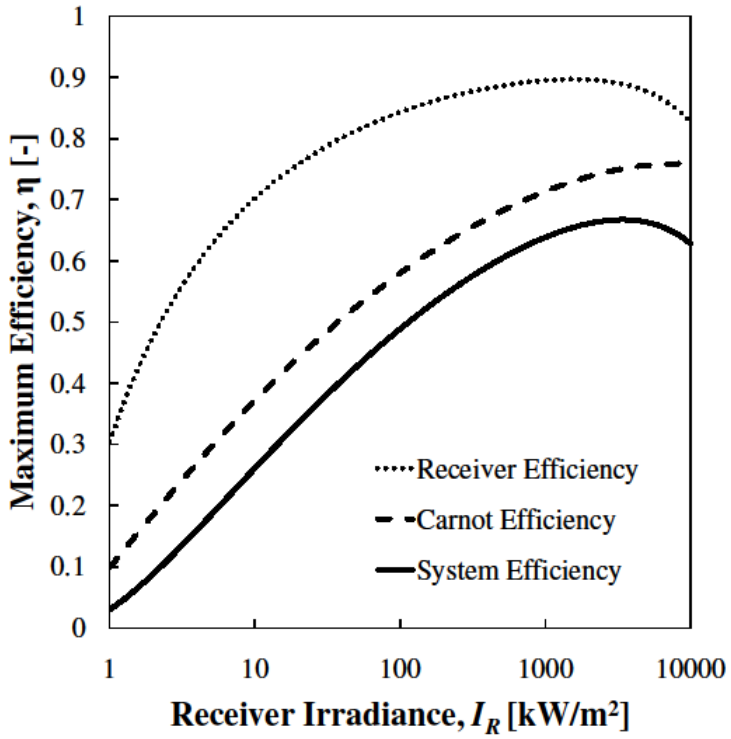

Fig. 4. System efficiency at optimal receiver temperature versus receiver irradiance

As receiver irradiance initially increases, the efficiency of the receiver increases as losses become less significant relative to the increasing receiver irradiance. Further increases in receiver irradiance result in a decreasing receiver efficiency factor and eventually Carnot factor, due to the increasing temperature differences between the receiver and the high temperature working fluid and also the low temperature working fluid and ambient. The presence of an optimal level of receiver irradiance is clear, although the question remains as to whether this optimal value is within the range of achievable values for receiver irradiance in real systems.

The solar thermal system's efficiency may also be plotted against the receiver's overall heat transfer coefficient (HTC) at a fixed value of receiver irradiance (again choosing receiver and condenser thermal resistances to be equal). As HTC increases, the optimal receiver temperature decreases whilst system efficiency increases. This highlights the importance of high heat transfer coefficients within heat exchangers to maximise system efficiency and also minimise the temperature at which the solar receiver must operate.

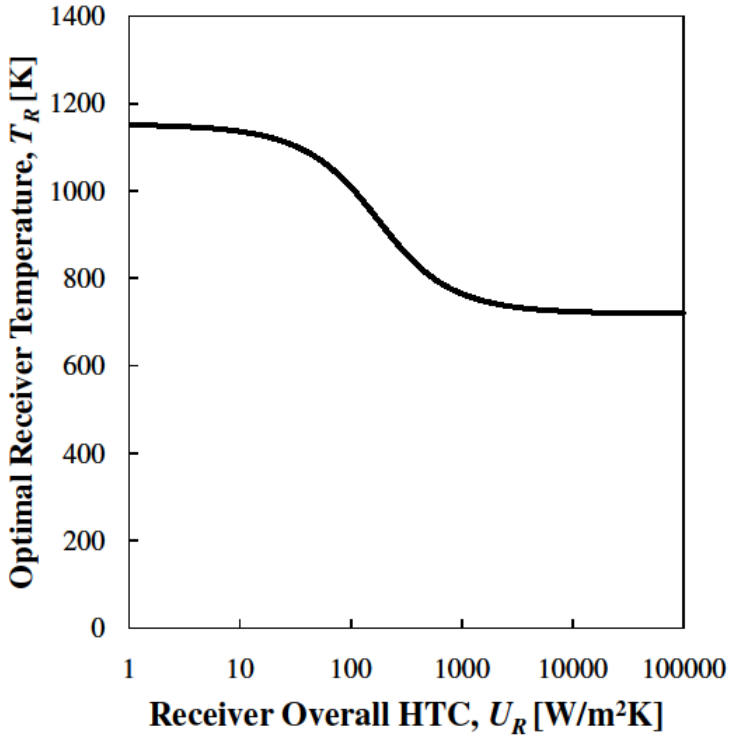

Fig. 5. Optimal receiver temperature versus receiver overall heat transfer coefficient, I_R = 100 kWm^{-2}

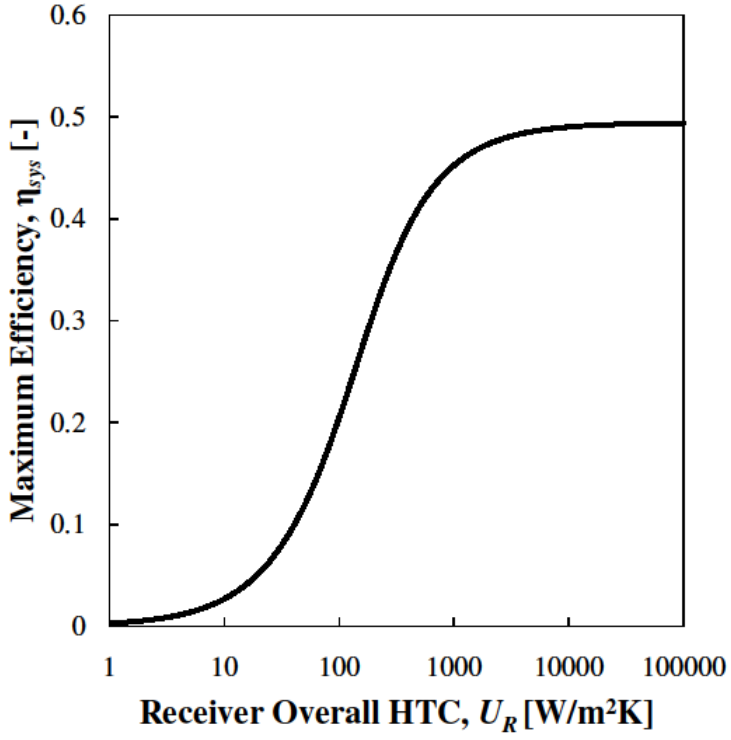

Fig. 6. System efficiency at optimal receiver temperature versus receiver overall heat transfer coefficient, I_R = 100 kWm^{-2}

As high values of HTC are approached, the system behaviour tends towards that of a Mueser engine (Fig. 1) since the thermal resistances of the receiver and condenser become negligible. At low values of HTC, the thermal resistance associated with radiative heat transfer becomes small compared to those of the receiver and condenser and the system begins to behave like a Curzon-Ahlborn engine [2-4].

3.2 Rankine Cycle Solar Tower and Trough Facilities

The model developed is now applied in an approximate manner to real solar tower and trough facilities. Two implementations are considered; one involving direct steam generation within the receiver and the other involving a service fluid of molten salts that transfers heat from the solar receiver to a steam generator. In each case, a constant temperature difference of 15 K is assumed across the condenser. The type of solar tower treated is that of an external receiver, whilst the trough is parabolic and heats a flow of fluid through a vacuum insulated pipe. Convection is deemed to be negligible in the case of the solar trough and a value of 0.9 is applied for the transmissivity of the outer tube. For the solar tower, convection is modelled as buoyancy driven flow over a vertical cylinder. The convection coefficient calculated by Wagner [10] based on correlations by Siebers & Kraabel is employed. The receiver is modelled as a grey body and absorptivity/emissivity is assigned a value of 0.9. As the receiver operates at higher temperature, the benefits of employing a selective surface coating decrease, since the optimal cut-off wavelength tends towards infinity. see [5]. The collector efficiency is set to 60% in the case of the solar tower and 75% in the case of the solar trough [12]. The ambient temperature is fixed at 300 K.

$$\bar{h}_{conv} \approx \frac{T_R}{60} + \frac{5}{3}, \qquad (20)$$

In the case of direct steam generation, a value of 15 kWm^{-2} is employed for the receiver overall heat transfer coefficient. The incorporation of a service fluid consisting of molten salts within the solar thermal system adds a further layer of detail. Heat is transferred from the receiver to the molten salts and then from the salts to the working fluid (water). In practise there would be a temperature drop in the molten salts during transmission and storage. This temperature drop is not modelled in this case. Such temperature drops would have the effect of driving the optimal receiver temperature to a higher level. Fig. 6 below describes the model employed for molten salts systems.

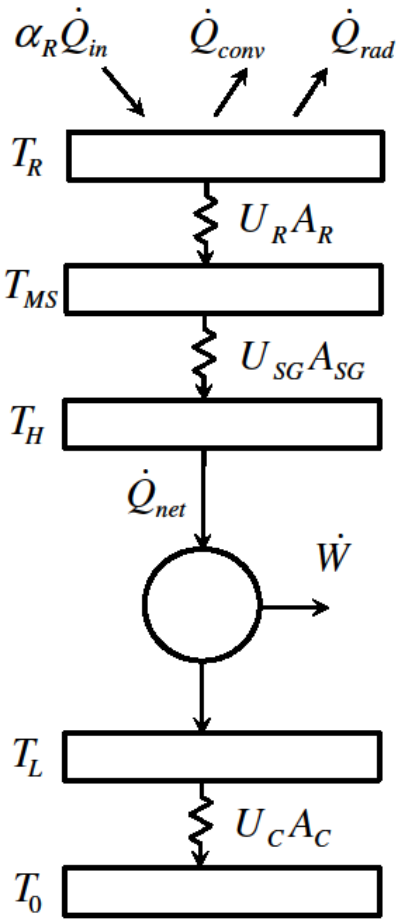

Fig. 6. Simplified model of a solar thermal plant operating with a service fluid

The convection coefficient associated with the heating and cooling of molten salts within a pipe is taken to be 1 kWm^{-2}, a representative convective coefficient for a fluid of 45% $NaNO_3$ – 55% KNO_3. For the purposes of this analysis, the thermal resistances associated with heat transfer from the receiver to salts and from the salts to steam are chosen to be equal for both the solar tower and the solar trough.

The optimal receiver temperatures and maximum system efficiencies of solar tower and solar trough systems are now plotted.

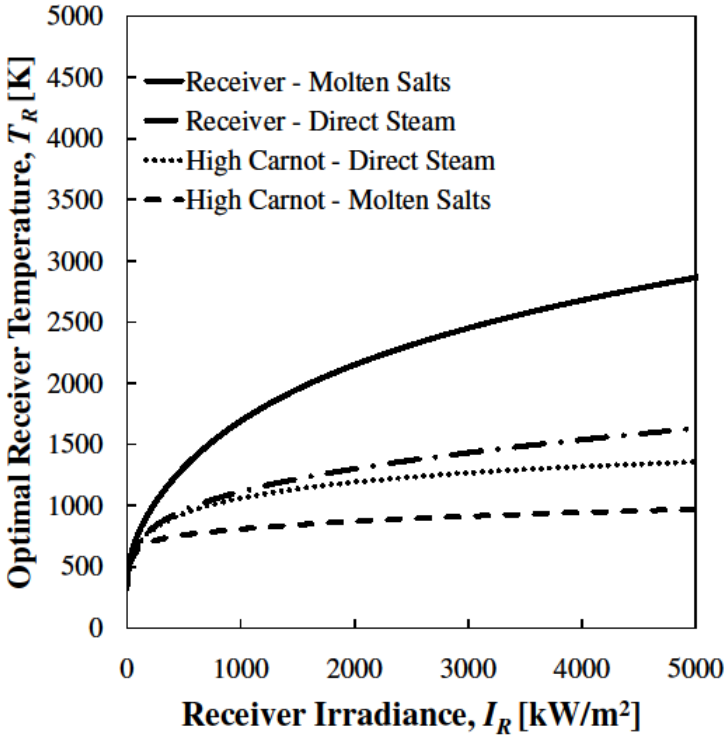

Fig. 8. Optimal receiver temperature versus receiver irradiance for a solar tower system

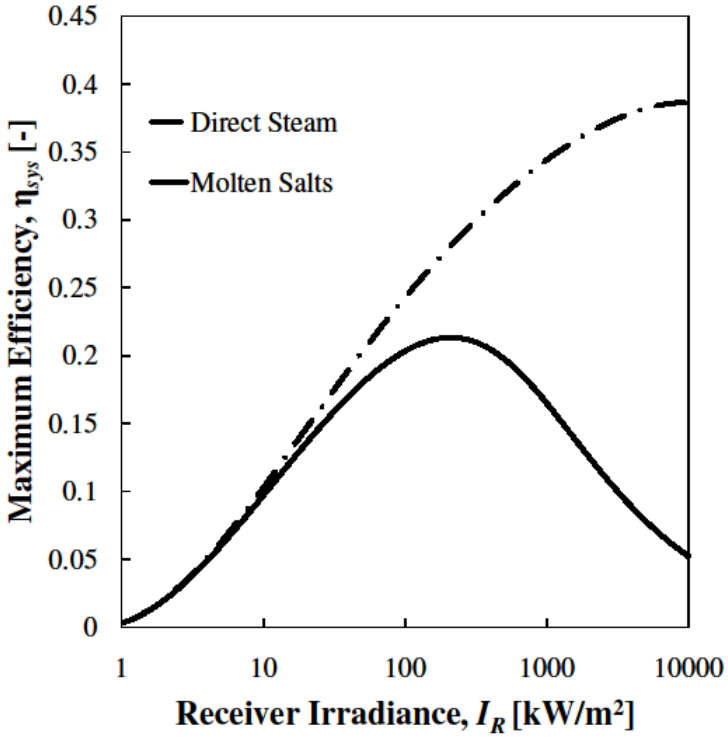

Fig. 9. System efficiency at optimal receiver temperature versus receiver irradiance for a solar tower system

The level of receiver irradiance achieved with current solar tower technologies does not go far beyond 1000 kWm^{-2}. In Fig. 9 it is seen that the difference in temperature between receiver and the high Carnot temperature becomes extremely large where a molten salt service fluid is used. The mean temperature of the molten salts would lie between that of the receiver and the high Carnot temperature. The use of the employed values of thermal resistance is inaccurate at these temperatures since no such systems are in existence. In order to achieve optimal receiver

temperatures at high levels of receiver irradiance a Brayton, Stirling or super-critical Rankine cycle would be required. One important conclusion is that peak efficiency for external receiver solar towers employing a service fluid of molten salts is reached at a much lower level of receiver irradiance than for direct steam. As the heat input to the heat engine increases, the temperature drop between the receiver and Carnot top temperature rises very rapidly, thus eroding system efficiency. Moreover, if one chooses to operate beyond the optimal level of receiver irradiance, the optimal receiver temperature will continue to rise, thus increasing the challenges involved in the receiver's thermal design.

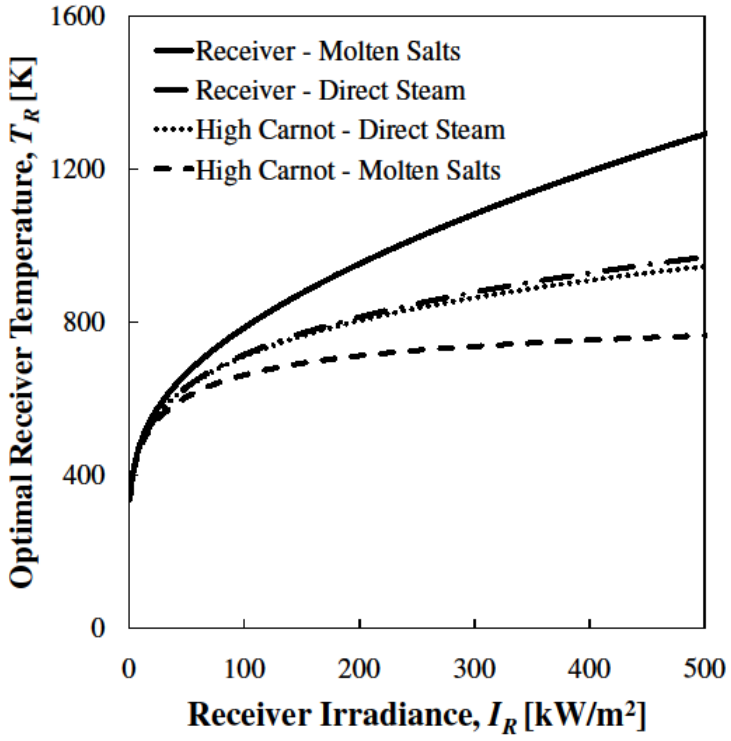

Fig. 10. Optimal receiver temperature versus receiver irradiance for a solar trough system

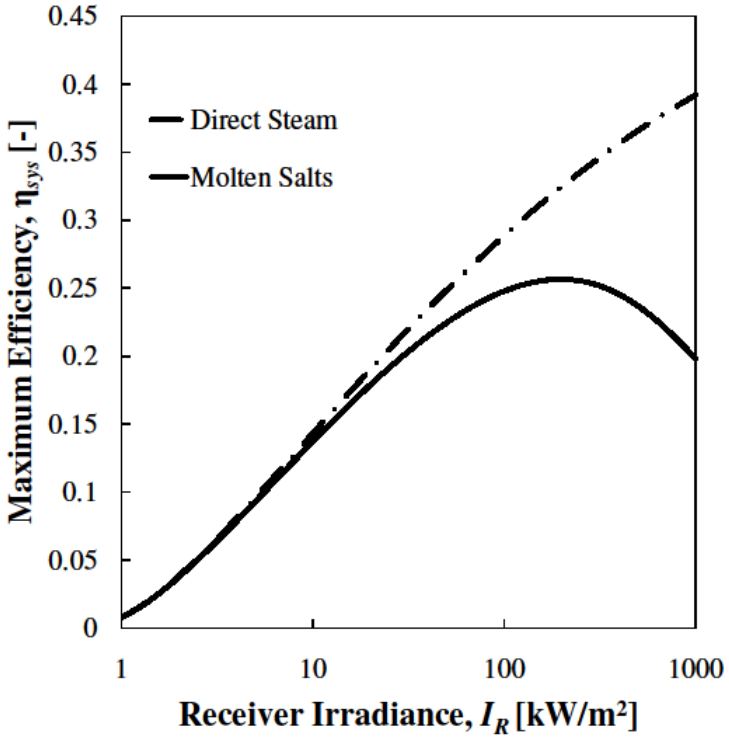

Fig. 11. System efficiency at optimal receiver temperature versus receiver irradiance for a solar trough system

Typically solar trough systems offer improved an improved collector efficiency compared to solar towers but operate at much lower levels of receiver irradiance, often below 100 kWm^{-2}. At this level, the optimal receiver temperature for solar trough systems is around 350 °C. At sufficiently low receiver irradiance, the use of a sub-critical Rankine cycle may be optimal. Again, when employing a service fluid of molten salts, there is little advantage to operating beyond a receiver irradiance of about 200 kWm^{-2}.

5. Conclusions

The impact of receiver irradiance and temperature upon the solar-to-electric efficiency of a generic solar thermal system is investigated. Increasing values of thermal resistance in the receiver and condenser and increasing values of heat transfer rate into the heat engine are shown to decrease the Carnot efficiency of the heat engine. As thermal resistances and receiver irradiance increase, the optimal receiver temperature is shown to increase. The performance of Rankine cycle direct steam and molten salts solar tower and solar trough plants are compared. The optimal level of receiver irradiance is found to occur at about 200 kWm^{-2} for solar tower and solar trough systems employing a service fluid of molten salts. The optimal receiver temperatures calculated suggest the use of sub-critical Rankine cycles for solar trough plants, but super-critical Rankine cycles for solar tower plants.

Acknowledgments

The first author would like to thank the US Department of State for funding through the Science and Technology PhD program.

Nomenclature

Letter Symbols

f radiative face factor, dimensionless

$\bar{h}$ convective heat transfer coefficient, W/(m^2 K)

I_R receiver irradiance, W/m^2

$\dot{q}_s$ insolation per unit collector area, W/m^2

$\dot{Q}$ rate of heat transfer, W

R thermal resistance, K/W

T temperature, K

$\dot{W}$ rate of work, W

X geometric concentration factor

Greek symbols

α absorptivity, dimensionless

ε emissivity, dimensionless

η thermal efficiency

σ Stefan-Boltzmann radiative constant

Subscripts

f radiative face factor, dimensionless

C condenser

Carnot Carnot

coll collector

conv convective

H high Carnot

in incident

L low Carnot

net net

R receiver

rad radiative

S solar

sys system

0 ambient

References

[1] Muser, H. Behandlung von elektronenprozessen in halbleiter-randschichten. Zeitschrift fur Physik 1957;148:380-390.

[2] Novikov I. The efficiency of atomic power stations (A review). Atomnaya Energiya 1957;11:409-412.

[3] Chambadal P. Les Centrales Nucleaires. Paris, France: Armand Colin; 1957;41-58.

[4] Curzon F, Ahlborn B. Efficiency of a Carnot engine at maximum power output. American Journal of Physics 1975;43:22-24.

[5] De Vos A. Thermodynamics of solar energy conversion. Weinheim, Germany: Wiley-VCH; 2008.

[6] Navarrete-Gonzalez T, Rocha-Martinez J, Angula-Brown F. A Mueser–Curzon–Ahlborn engine model for photothermal conversion. J. Phys. D: Appl. Phys. 1997;30:2490-2496.

[7] Rocha-Martinez J, Navarrete-Gonzalez T, Angula-Brown F. A simple relationship between the sunlight concentration factor and the thermal conductance in a class of photothermal engines. J. Phys. D: Appl. Phys. 1998;31:1742-1744.

[8] McMahan A, Klein S, Reindl D. A finite-time thermodynamic framework for optimizing solar-thermal power plants. Journal of Solar Engineering 2007;129:355-362

[9] Odeh S, Morrison G, Behnia M. Modelling of parabolic trough direct steam generators. Solar Energy 1999;62:395-406.

[10] Wagner, M. Simulation and predictive performance modeling of utility-scale central receiver system power plants. Madison, Wisconsin: University of Wisconsin-Madison, 2008.

[11] Siebers D, Kraabel J. Estimating convective energy losses from solar central receivers (4th edition). Albuquerque: Sandia National Laboratories; 1984 No.: *SAND84-8717*

[12] Assessment of Parabolic Trough and Power Tower Solar Technology Cost and Performance Forecasts. Chicago, Illinois: Sargent & Lundy LLC Consulting Group: 2003. Subcontract No.: LAA-2-32458-01